



ORIGINAL ARTICLE

Important aspects in experimental *versus* numerical comparative analysis in pile caps

Aspectos importantes em análise comparativa experimental versus numérico em blocos sobre estacas

Gustavo Leardini Luchesi^a Ricardo de Paula Randi^a Leandro Mouta Trautwein^a Luiz Carlos de Almeida^a ^aUniversidade Estadual de Campinas – Unicamp, Departamento de Estruturas, Campinas, SP, BrasilReceived 01 December 2021
Accepted 25 January 2022

Abstract: Research with emphasis on comparative analysis between experimental models *versus* numerical models in pile caps tend to present discrepancies in stiffness between models. The present paper numerically analyzes pile caps on two piles, emphasizing parameters that have direct influence on the responses of the simulated models, especially in terms of stiffness. Among the parameters evaluated in this paper, we note the following: boundary conditions applied to the base of the piles; the use of interface elements in the simulation of contact between materials; and the influence of pile cap width. The analyzed results are related to failure load, displacements, load *versus* displacement curves, stress flows, and cracking panoramas. The findings demonstrate that the parameters analyzed here have direct influence on the results of the numerical models when compared with the experimental results.

Keywords: pile caps, reinforced concrete, finite elements, numerical modeling, comparative analysis.

Resumo: Pesquisas com ênfase em análises comparativas entre modelos experimentais *versus* modelos numéricos em blocos sobre estacas tendem a apresentar discrepâncias nas rigidezes entre os modelos. O presente trabalho analisa numericamente blocos apoiados sobre duas estacas, enfatizando parâmetros que influenciam diretamente as respostas dos modelos simulados, principalmente no quesito da rigidez. Dentre os parâmetros avaliados nesse trabalho, destacam-se: as condições de contorno aplicadas na base das estacas, a utilização de elementos de interface na simulação do contato entre materiais e a influência da largura do bloco. Os resultados analisados são relativos à carga de ruptura, aos deslocamentos, às curvas carga *versus* deslocamento, aos fluxos de tensões e aos panoramas de fissuração. Os resultados encontrados demonstram que os parâmetros aqui analisados influenciam diretamente os resultados dos modelos numéricos quando comparados a resultados experimentais.

Palavras-chave: blocos sobre estacas, concreto armado, elementos finitos, modelagem numérica, análise comparativa.

How to cite: G. L. Luchesi, R. P. Randi, L. M. Trautwein, and L. C. Almeida. "Important aspects in experimental *versus* numerical comparative analysis in pile caps" *Rev. IBRACON Estrut. Mater.*, vol. 15, no. 5, e15502, 2022, <https://doi.org/10.1590/S1983-41952022000500002>

1 INTRODUCTION

Pile caps are structural elements that transfer load between the superstructure (columns) and the infrastructure (foundation). They are usually buried, making visual inspection difficult, and, therefore, it is important to understand the behavior of this structural element in the Ultimate and Service Limit States.

Corresponding author: Ricardo de Paula Randi. E-mail: ricardo_randi@hotmail.com

Financial support: None.

Conflict of interest: Nothing to declare.

Data Availability: The data that support the findings of this study are available from the corresponding author, [G.L. Luchesi].



This is an Open Access article distributed under the terms of the Creative Commons Attribution License, which permits unrestricted use, distribution, and reproduction in any medium, provided the original work is properly cited.

According to ABNT NBR 6118/2014 [1], pile caps are classified as rigid and flexible, being designed by the Strut-and-Tie Model Method or truss analogy method (Bending Theory), respectively. Note, therefore, that prior knowledge of pile cap dimension is essential for its designing

The Strut-and-Tie Model Method is based on the work of Blévoit and Frémy [2], which tested 116 pile caps supported on two, three, four, five and six piles. The authors found that the internal mechanism of a foundation pile cap can be idealized by a spatial truss composed of tension and compression bars. Tension bars represent the result of the tension forces and based on them the principal reinforcements are designed. Compression bars represent compressed struts and are generally inclined, defined from the column/pile cap interface (upper node) to the pile cap/pile interface (lower node).

After publication of the work of Blévoit and Frémy [2], authors such as Mautoni [3], Taylor and Clarke [4], Adebar et al. [5], Schlaich and Schafer [6], and Sam and Iyer [7] performed experimental and numerical research on the subject and suggested more refined models for the Strut-and-Tie Method. It is noted, among other observations, that several authors conclude that pile caps reach ruin by crushing of concrete in nodal regions, after the appearance of a rupture plane inclined towards the compression struts, a phenomenon influenced by the concrete bursting effect.

Normative codes such as ACI 318:19 [8], CEB-FIP 2010 [9], CSA Standard 2019 [10] and ABNT NBR 6118/2014 [1] itself present recommendations for employing the Strut-and-Tie Method in the designing of pile caps. It should be noted that there are many divergences about the behavior of pile caps and the idealization of designing models, especially regarding strut geometry, column cross section, pile spacing, loading type (eccentric or centered).

More recently, Delalibera [11], Buttignol [12], Munhoz [13], Barros et al. [14] and Randi [15] performed researches with numerical emphasis that demonstrate the complexity of replicating experimental tests in numerical models.

Delalibera [11] parametrically analyzed pile caps and found disparities in the stiffness of numerically simulated experimental specimens. According to the author, the greater stiffness of the numerical model occurs due to accommodation of the experimental models at the beginning of the test, by considering the perfect adhesion between the reinforcement bars and concrete and, finally, by assuming a perfect connection between the piles and the pile caps.

Buttignol and Almeida [16] numerically analyzed pile caps on two piles varying the degree of vertical restriction at the base of the piles. The author found that variation in support connection has direct influence on pile cap behavior, having a non-negligible influence on pile cap stiffness.

Barros et al. [14] performed nonlinear numerical analyses in four pile caps on two piles based on the experimental tests of Delalibera [11] and found disparities in the results regarding the displacements of the models, and the numerical models presented lower displacements than those obtained experimentally, in addition to greater stiffness.

Randi et al. [17] performed numerical analyses based on the experimental tests of Munhoz [13]. The author observed, when comparing the load *versus* displacement curves, that the stiffness of the numerical models in phases of the test prior to the opening of the first visible cracks is greater than that of the experimental models.

In general, several authors conclude that numerical models of pile caps tend to present greater stiffness and, consequently, smaller displacements. Relatively to the behavior of the pile caps analyzed numerically, the results are like the experimental tests.

It is observed that several parameters influence the behavior and stiffness of pile caps analyzed numerically, among them the boundary conditions of the pile base as shown by Buttignol and Almeida [16], the connection between piles and pile caps as observed by Delalibera [11], corroborated by Randi [15].

2 JUSTIFICATION

The main justification of this paper is the observation of small divergences presented in simulations of pile caps through reference experimental tests, mainly in the differences in stiffness between the models. The objective is to judiciously improve the results of future researches with an experimental *versus* numerical emphasis. It is also observed that there are few researches on pile caps in which the models are analyzed with the minimum side flaps indicated by the specialized literatures and normative codes, tests with pile caps with widths equal to the column are more common.

3 METHODOLOGY

The numerical models analyzed in this paper are based on two-pile caps experimentally tested by Munhoz [13], designed according to the Strut-and-Tie Method suggested by Blévoit and Frémy [2] and according to the recommendations of ABNT NBR 6118:2003 [18]. It should be noted that these models have no side flap, and the pile cap width dimensions are close to the side dimensions of the piles and columns.

The numerical simulations were conducted with the aid of the computer program ATENA3D version 5.4.1 distributed by the company Cervenka Consulting. The program is based on the Finite Element Method and enables the solution of nonlinear problems in reinforced concrete elements. The models' pre-processing – phase of defining geometry, materials, monitoring points, and analysis method – was performed with the aid of the computer program GID version 10.0.9. The processing and post-processing phases were performed in ATENA3D itself.

Initially, a parametric numerical analysis was performed, changing the boundary conditions at the base of the piles, comparing the results of the failure loads and displacements of the numerical models with the reference experimental results. Subsequently, an analysis was performed, changing the connection between the piles and the pile caps. This analysis used interface elements, available in the ATENA3D computer program, and again the failure loads and displacements were compared, in addition to the stress flows within the pile caps. Through the definition of the most suitable model, a comparison was made between the reference experimental models and the numerical models, covering, in addition to failure loads and displacements, the results related to cracking panoramas.

Finally, to evaluate the influence of pile cap width on its behavior, it was performed a comparative numerical analysis between simulated models considering the side flap *versus* simulated models without the side flap. At this point, the results related to failure loads, displacements and stress flows within the pile cap were also compared.

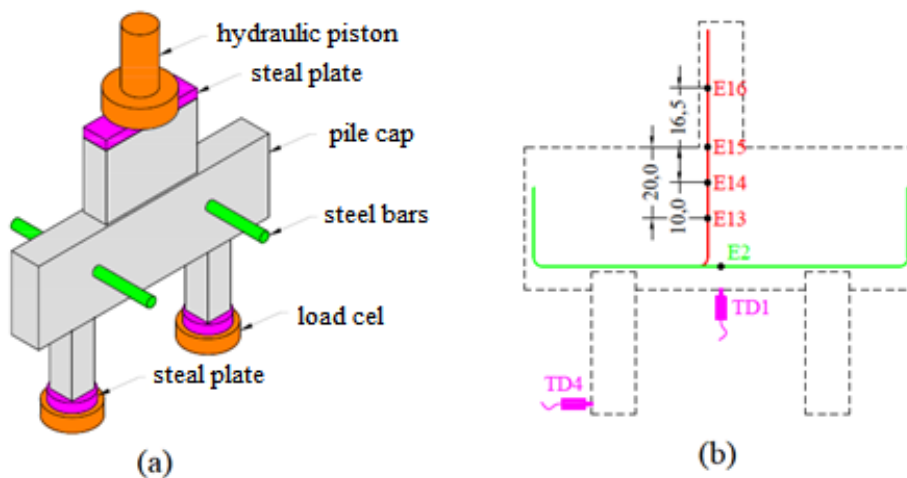
4 DESCRIPTION OF REFERENCE EXPERIMENTAL MODELS AND NUMERICALLY SIMULATED MODELS

It should be noted that a comparative analysis was performed between the three-dimensional numerical models presented in this paper with the two-dimensional numerical models presented in Randi [15]. The reference experimental models are the same as in Munhoz [13], and this step was performed to validate the numerical results. The results of this analysis will be discussed briefly here and are presented in full in Luchesi [19].

4.1 Reference experimental models

Munhoz [13] tested four different series of pile caps on two piles, defined according to different column sections and reinforcement ratios. The columns have a section of 12.5 x 12.5 cm, 12.5 x 25 cm, 12.5 x 37.5 cm, and 12.5 x 50.0 cm and a height of 35.0 cm. The piles have a square section of 12.5 x 12.5 cm and a height of 40.0 cm, with 5.0 cm embedded in the pile caps. The pile caps are standardized with a height of 40.0 cm, compression strut angle was set at 55°, while pile spacing varied according to the series studied as a function of column section. Regarding thickness, the pile caps have 15.0 cm and the columns and piles have 12.5 cm, that is, they do not have a side flap.

The tests were performed using a universal testing machine with a load capacity of 2500.0 kN until the experimental models break. Figure 1 presents a schematic drawing of the experimental tests.

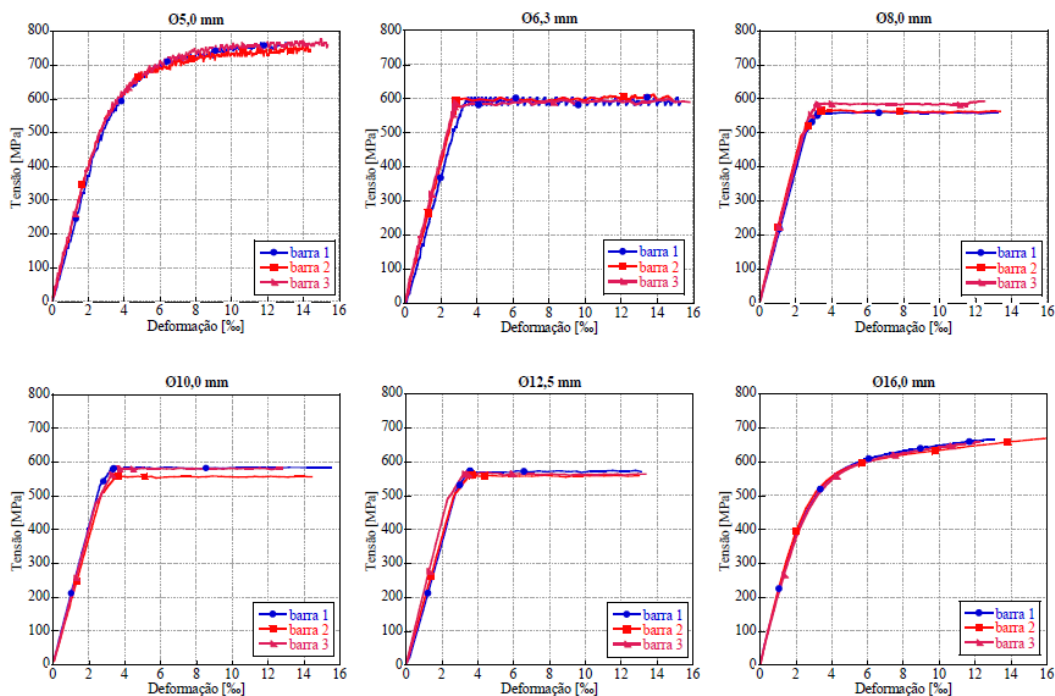


The nomenclature of the experimental models was defined based on the pile cap length and column reinforcement ratio. For example, in model B127P500R2.5, the letter B refers to pile cap length (127.0 cm), the letter P refers to the column side (50.0 cm), and the letter R refers to the column reinforcement ratio (2.5%). Therefore, 12 different pile cap models were experimentally analyzed: B110P125R1, B110P125R2.5, B110P125R4, B115P250R1, B115P250R2.5, B115P250R4, B120P375R1, B120P375R2.5, B120P375R4, B127P500R1, B127P500R2.5 and B127P500R4.

Concrete properties were determined through compression tests of specimens (10.0 x 20.0 cm) and two different strengths were used for column/pile cap and piles, being 25 MPa and 50 MPa, respectively.

The experimental models had monitoring points (strain gauges) placed along the longitudinal bars at four different heights of the column, in the center of the tie bars, and in the center of the top of the piles. Displacement transducers were also allocated. Figure 1 presents, for a pile cap of the B110 series, the location of the most important monitoring points and displacement transducers for the analysis presented in this paper. It should be noted that in experimental tests there are other monitoring points that will not be addressed here.

The mechanical properties of the reinforcement steel were determined through tensile tests on bars with a length of 100.0 cm for each diameter used. ATENA 3D software allows the user to input stress *versus* strain data to simulate steel behavior, the authors used this tool to characterize the steel reinforcement. The mechanical properties are presented in Figure 2.



A more detailed description of the material properties, the positions of reinforcement in columns/pile caps/piles, and the performance of experimental tests can be found in Randi [15], Luchesi [19] and originally in Munhoz [13].

4.2 Numerical models

The numerical models have the same geometry, material properties, and position of monitoring points and displacement transducers as the reference experimental models. The simulation of the models was performed using the computer program ATENA3D with a non-linear solution based on the Newton-Rhapson method.

The constitutive model used to simulate the concrete material was *CC3DNonLinearCementitious2*, being a plastic fracture model called Fracture – Plastic Constitutive Model, described in Cervenka and Papanikolaou [20]. This model enables the simulation of phenomena associated with the behavior of concrete such as plasticization in compression and fracture in tension. In compression, the material behaves non-linearly with hardening and softening based on the

rupture surface of Menetrey and William [21]. In tension, the nonlinear behavior for fracture is based on the formulation of Rashid [22] for the incorporated crack and on the crack band model of Bazant and Oh [23]. The tensile rupture criterion adopted is that of Rankine [24] together with the cohesive model by the exponential softening function of Hordijk [25].

For the reinforcements, we used a discrete model that simulates the steel bars incorporated in the concrete material. This model considers the Von Mises plasticity model. Steel bars assume a uniaxial stress state based on Hooke's Law. The ATENA3D computer program enables the definition of stress *versus* strain curves of steel from test data. In this case, we used the tensile rupture test data provided by Munhoz [13].

The interface elements simulate the connection between different materials, such as steel plates and concrete, or a joint between two concrete segments in the case of the pile cap/pile connection. These elements present a constitutive model that simulates the contact and stiffness between different materials and are based on the Mohr-Coulomb criterion, considering maximum tensile stress (f_t), cohesion (c), and friction (ϕ).

The parameters of normal stiffness (K_{nn}) and transverse stiffness (K_{tt}) determine the deformations and displacements that occur in interface elements. For a proper simulation of interface elements, the minimum normal stiffness and the minimum transverse stiffness of the material must be defined, which are used for a numerical assumption to maintain the continuity of the simulated element equilibrium after interface material rupture and, according to Cervenka et al. [26], should be around 0.001 times the maximum value of the initial rigidities. Figure 3 presents the behavior of the interface elements according to Cervenka et al. [26].

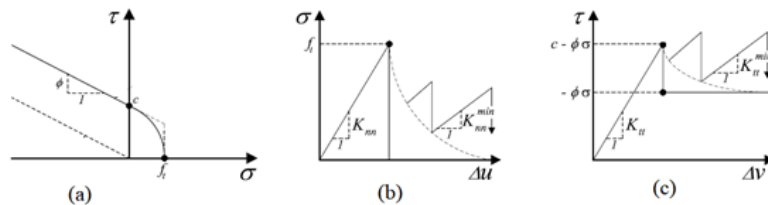


Figure 3. (a) Rupture surface of the interface element. Behavior of the interface model subject to normal stress (b) and shear stress (c). Adapted from Cervenka et al. [26].

The numerical models were simulated by adopting a discretization of a finite element mesh with a maximum size of 3.0 cm. Figure 4 presents the discretized model and the types of elements used for each material. As in the reference experimental models, steel plates were placed at the top of the column and at the base of the two piles.

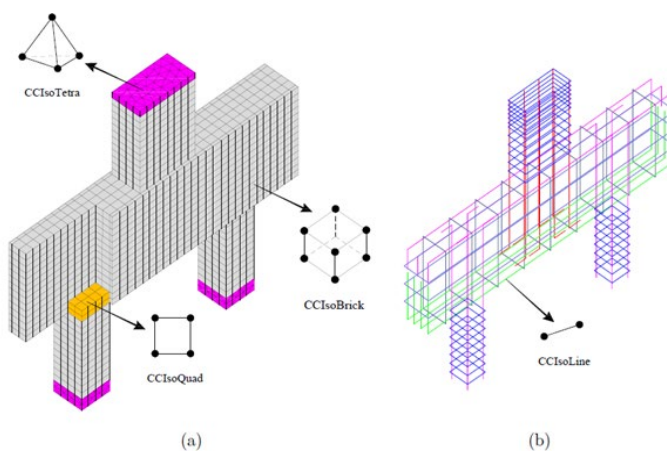


Figure 4. Discretization of solid (a) and linear (b) elements

The loading in the numerical models was simulated with the imposition of a displacement in the vertical direction, uniformly distributed over the entire surface of the plate present at the top of the column, incrementally through 200 steps. The maximum values of these displacements were based on the experimental results of Munhoz [13].

4.2.1 Numerical models of parametric numerical analysis of boundary conditions

To verify the influence of boundary conditions on the behavior of pile caps on piles simulated numerically, four different models were analyzed, varying the connections at the base of the pile. The models are based on the reference experimental models B100R4 and B127R2.5. The nomenclatures CC1, CC2, CC3, and CC4 were added in the nomenclature of the models. Figure 5 presents a schematic drawing of the boundary conditions used.

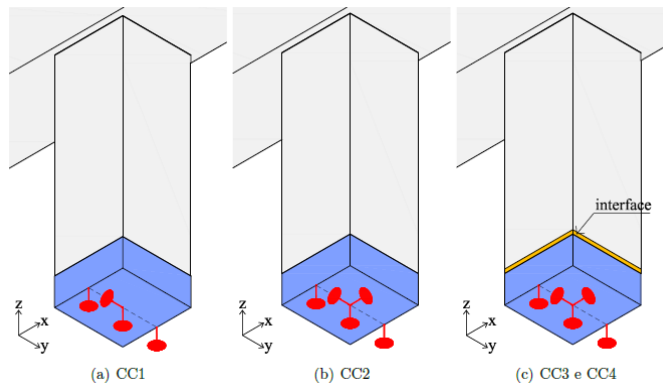


Figure 5. Boundary conditions at the base of the piles

For all models, the vertical displacement was restricted in the Z direction in the central line of the support steel plates and in the Y direction. At the top of the column, there is also a steel plate, with displacement restrictions in the X and Y directions.

For the boundary condition of models B110R4CC1 and B127R2.5CC1, horizontal displacement constraints in the X direction were not considered, simulating a roller support on the steel plates of the supports. For models B110R4CC2 and B127R2.5CC2, horizontal displacement in the X direction was restricted, only in the central point of the support, simulating a fixed support. For models CC1 and CC2, we adopted a rigid connection between the base of the piles and the top of the steel plate.

Boundary conditions for models CC3 and CC4 are identical to those for models CC2. However, in these models, interface elements with different mechanical properties were used in the connection between the base of the piles and the top of the steel plate. It is worth noting that, in the connection between the top of the column and the base of the steel plate, where the loading was applied, there are also interface elements. The mechanical properties of the interface elements are present in Tabel 1.

Table 1. Mechanical properties and position of interface elements of models CC3 and CC4

Model/Position	Knn	Ktt	ft	Friction	Cohesion	Knn,min	Ktt,min
	(MPa)	(MPa)	(MPa)		(MPa)	(MPa)	(MPa)
CC3 and CC4 Column	1.0×10^7	1.5×10^3	0.1	0.3	1.0	1.0×10^4	1.5
CC3 - Piles	2.0×10^6	2.0×10^6	0.1	0.3	1.0	2.0×10^3	2.0×10^3
CC4 - Piles	2.0×10^4	1.5×10^3	0.1	0.3	1.0	2.0×10^1	1.5

To improve the numerical models and reach more accurate results when compared to Munhoz (2014) experiments, the mechanical properties of interface elements were modified. As mentioned in section 4.2, Cervenka et al. [26] presents a theoretical base to simulate the interface. However, the authors could not reach satisfactory results using the theoretical calculations presented in Cervenka et al. [26]. Modifications were performed for the results presented in Tabel 1 and Tabel 2.

4.2.2 Numerical models of the parametric numerical analysis of the connection between pile caps and piles

In the reference experimental models, the concreting was performed in two distinct steps. In the first step, were concreted the piles with a compression strength of 50 MPa and, in the second step, the pile caps and columns with a compression strength of 25 MPa, and the piles were embedded 5.0 cm inside the pile caps.

Considering that concreting joints were created between the piles and pile caps, models B110R4 and B127R2.5 will be analyzed in two different cases of connection. The first without interface elements, that is, a rigid connection, and the second with interface elements in the contact between pile cap/pile. Figure 6 presents the geometry of the interface elements and Tabel 2 presents the mechanical properties of these elements. The nomenclatures LR (Rigid Connection) and LI (Connection with Interface) will be added to the final nomenclature of the pile caps analyzed numerically in this step, thus obtaining the following: B110R4LR, B110R4LI, B127R2.5LR, and B127R2.5LI.

Table 2. Mechanical properties of interface elements in models B110R4LI and B127R2.5LI

Position	Knn	Ktt	ft	Friction	Cohesion	Knn,min	Ktt,min
	(MPa)	(MPa)	(MPa)		(MPa)	(MPa)	(MPa)
Column	1.0×10^7	1.5×10^3	0.1	0.3	1.0	1.0×10^4	1.5
Piles	1.0×10^7	1.0×10^7	2.5	0.5	6.0	1.0×10^4	1.0×10^4

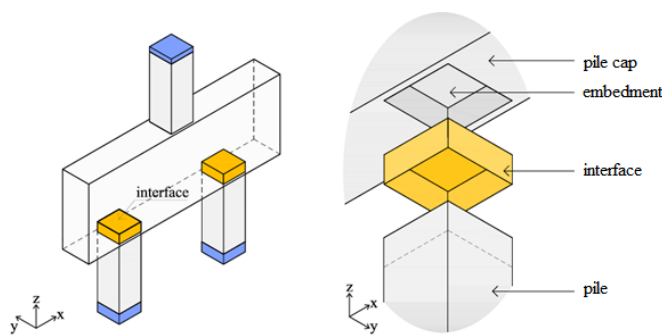


Figure 6. Geometry of interface elements used in the pile-pile cap connection

4.2.3 Numerical models for analyzing the influence of pile cap width

In general, pile caps on piles are tested experimentally without a side flap. The side flap is defined as a minimum distance between the face of the pile and the face of the pile cap, and it is usual in Brazil to use the minimum value of 15.0 cm, recommended by Alonso [27]. ABNT NBR 6118/2014 [1] presents no recommendation for determining pile cap width or pile coverage in relation to pile cap face.

Considering that the reference experimental models do not have a considerable side flap, two new models will be simulated. The reference experimental models B110P125R4 and B127P500R2.5 have a total width of 15 cm, which is the sum of 12.5 cm on the pile side plus 1.25 cm of flap for each side. These models will receive the index C1.25 at the end of their nomenclature.

For the numerical models, 15 cm of flap will be added for each side, obtaining a total width of 42.5 cm, and the indexes C15 will be added to the nomenclature. The stirrups that constitute these pile caps were increased in the direction of the pile cap width by 27.5 cm, keeping the initial reinforcement coverage. To control cracks opening and increase flexural strength of the pile-cap, two bars with 10.0 mm in diameter will be added in the four models studied. The bars of the upper reinforcement were spaced equally in the direction of the pile cap width. Figure 7 illustrates the differences between the models mentioned above. In the models showed in Figure 7, seven 12,5 mm steel reinforcements were disposed in each face of the columns and four 12,5 mm steel reinforcements were disposed in the piles.

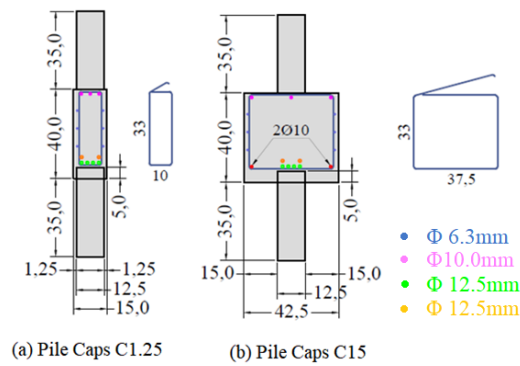


Figure 7. Cross section of models (a) C1.25 and models (b) C15

5 RESULTS AND DISCUSSIONS

The results will be presented in three different steps. The first step will present the results of failure loads and displacements, measured in displacement transducers TD1 and TD4, relative to models with changes in boundary conditions and rigidities of interface elements. In this step, the stress flow inside the pile caps will also be discussed. The second step has a comparison between the reference experimental models and the numerical models that presented more consistent results through parametric analysis of boundary conditions. Finally, in the third step, the results of the analysis of influence of pile cap width will be discussed. It was observed that all models reached ruin by crushing of concrete in nodal regions, after the appearance of a rupture plane inclined towards the compression struts.

5.1 Results of numerical models with changes in boundary conditions and rigidities of interface elements

The results of failure loads (F_u) and displacements in transducers TD1 and TD4 of models CC1, CC2, CC3, and CC4 are presented in Tabel 3.

Table 3. Results for failure loads and displacement in transducers of experimental and numerical models with variation in pile connections

Model	B110R4		
	F_u	TD1	TD4
	(kN)	(mm)	(mm)
Experimental	590.7	2.78	0.18
B110R4CC1	583.5	1.39	1.80
B110R4CC2	602.4	1.44	0.16
B110R4CC3	612.3	1.49	0.17
B110R4CC4	596.8	2.41	0.72
Model	B110R2.5		
	F_u	TD1	TD4
	(kN)	(mm)	(mm)
Experimental	979.9	3.59	0.87
B127R2.5CC1	971.4	1.50	1.76
B127R2.5CC2	962.9	1.35	0.13
B127R2.5CC3	961.0	1.37	0.13
B127R2.5CC4	979.6	2.93	0.63

Figure 8 shows the results of failure load *versus* displacement in transducer TD1 for the two series of pile caps, B110R4 and B127R2.5. It is verified that the failure loads of the numerical models are close to the reference experimental model. However, it is observed that the displacements measured on the transducers vary significantly with different connections.

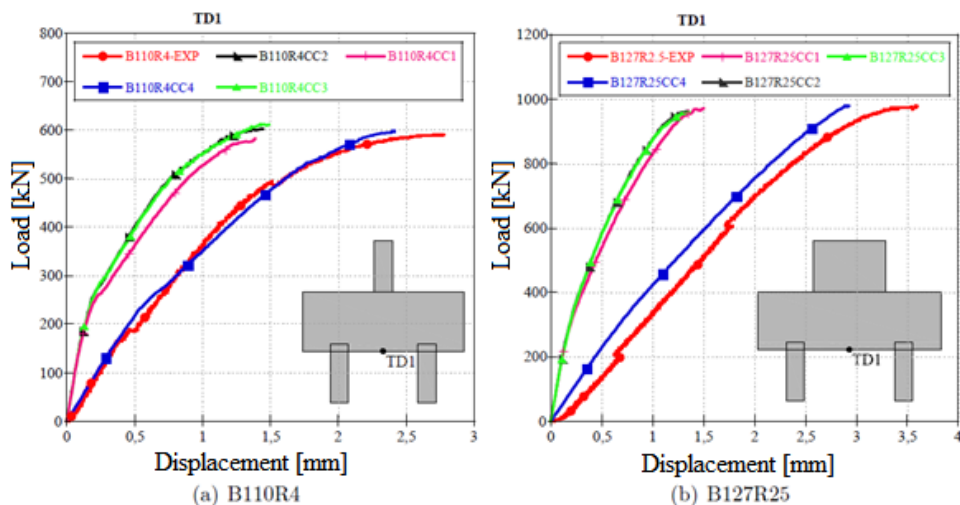


Figure 8. Load versus displacement [TD1] curves of the models of series B110R4 and B127R2.7 for analysis of boundary conditions

The numerical models CC1 and CC2 have no interface element in the contact between steel plate and pile, that is, the connection is rigid. The models CC3 have an interface element; however, the stiffness values used are high. It is noted, for these cases, that displacements in transducer TD1 presented a value well below the experimental results. On the other hand, the models CC4 were modeled with interface elements with lower stiffness and it is verified, by the results of Tabel 3, greater similarity to the results of the reference experimental models. It is noted, by Figure 8, that the curve of models B110R4CC4 and B127R2.5CC4 have stiffness closer to the experimental models.

Regarding horizontal displacement at pile base, measured by transducer TD4, it is verified that models CC1 that simulate a mobile support presented displacement results far above the experimental results. Models CC2 and CC3 of series B110R4, with horizontal displacement restriction, presented results very close to those of the reference experimental model, a fact not observed in the models of series B127R2.5. In the case of the model of series B127R2.5, model CC4 presented a more adequate result. These disparities in results corroborate the conclusions of researches about numerical simulations of pile caps supported on piles, referring to the complexity of replicating experimental tests in numerical models. Such results also demonstrate the differences in stiffness between experimental and numerical models.

The purpose of numerical simulations to evaluate the boundary condition of the models was to obtain satisfactory results in relation to the experimental models, that is, the purpose of this study was not to obtain identical results, but results that prove the similar behavior in relation to the experimental models for displacements and failure loads. Thus, the boundary condition of CC4 was chosen to simulate the supports at the base of the piles of future numerical models.

To evaluate the influence of the stiffness of the interface elements used in the pile cap-pile connection, the failure loads (F_u) and the displacements in the TD1 transducers were also evaluated. Tabel 4 presents these values.

Table 4. Results for failure loads and displacement in transducers of the experimental and numerical models with variation in pile cap/pile connection

Model	B110R4		
	F_u (kN)	$F_u, num / F_u, exp$	TD1 (mm)
Experimental	590.7	-	2.78
B110R4LR	656.0	1.11	2.36
B110R4LI	596.8	1.01	2.41
Model	B127R2.5		
	F_u (kN)	$F_u, num / F_u, exp$	TD1 (mm)
Experimental	979.9	-	3.59
B127R2.5LR	1130.0	1.15	3.30
B127R2.5LI	979.6	1.00	2.93

The use of interface elements in the pile cap/pile connection results in failure loads closer to those of the reference experimental models, a phenomenon also found by Buttignol [12].

Another important finding observed in the numerical simulations performed is related to the stress flow in the formation of the lower nodal region of the compression struts. The numerical models simulated with a rigid connection between pile cap and piles showed the formation of the lower nodal region with stresses involving the entire region of the piles embedded in the pile cap. Figure 9 presents the main stress flows of numerical models B110R4 and B127R25 for the different connections between pile cap and piles.

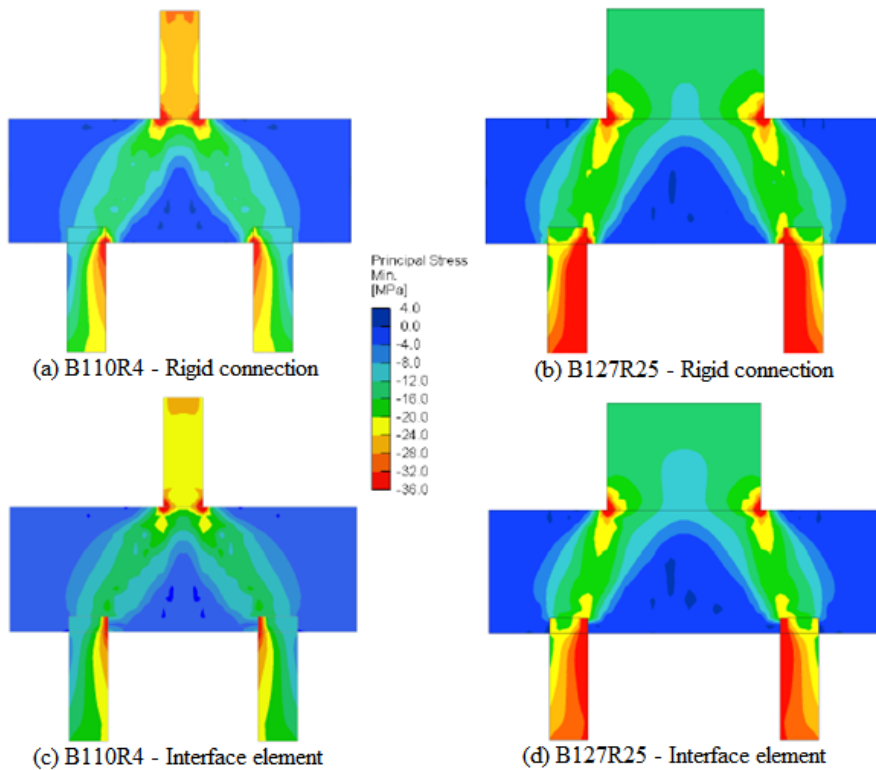


Figure 9. Influence of pile cap-pile connection on stress flow in numerical models (a) B110R4LR, (b) B127R2.5LR, (c) B110R4LI and B127R2.5LI

By analyzing Figure 9, it is found, in (a) and (b), that the stress concentration that characterizes the formation of the compression struts' lower node occurs on the piles' internal face, contrary to the Strut-and-Tie Model that considers the node to be formed at the pile head center.

It is also noted that the stress distribution in the contact region between pile cap and pile is distributed in different ways for the cases of rigid connection (Figure 9 – (a) and (b)) and connection with interface element (Figure 9 – (c) and (d)). The emergence of tensile stress on the pile external face is verified, proving that the pile cap tends to rotate on the piles due to the flexion and eccentricity of the lower node formation, which can cause detachment of concrete from the pile cap with pile, a fact also observed by Delalibera [11].

5.2 Reference experimental models *versus* numerical models

To validate the numerical modeling, we compared the results related to the failure loads, load *versus* displacement curves, and cracking panoramas of the experimental models B110P125R4 and B127P500R2.5 and the equivalent numerical models. It is noted that the numerical models discussed here consider the boundary condition adopted in CC4 models and pile cap-pile connection with interface element, which presented results more consistent with the experimental models, as discussed in item 5.1.

Table 5 presents the results for failure loads (F_u) and vertical displacements (δF_u) measured in transducer TD1 for failure load. The models with suffix EXP are the reference experimental models of Munhoz [13], the suffix 2D is related

to the two-dimensional modeling performed by Randi [15], and the suffix 3D is related to the three-dimensional modeling performed by Luchesi [19].

Table 5. Failure loads and vertical displacements of the models of series B110R4 and B127R2.5

Model	Series B110R4			
	Fu (kN)	Fu, num / Fu,exp	δFu (mm)	δFu, num / δFu,exp
B110R4-EXP	590.73	-	2.78	-
B110R4-3D	597.14	1.01	2.41	0.87
B110R4-2D	600.00	1.02	2.09	0.75
Model	Series B127R2.5			
	Fu (kN)	Fu, num / Fu,exp	δFu (mm)	δFu, num / δFu,exp
B127R2.5-EXP	979.88	-	3.59	-
B127R2.5-3D	979.64	1.00	2.93	0.82
B127R2.5-2D	1180.00	1.20	2.73	0.76

By analyzing Tabel 5, it is verified that the results related to failure loads were like the numerical models, except for model B127R2.5-2D. In relation to displacements, it is noted that the three-dimensional models presented displacements closer than the two-dimensional models. These observations demonstrate that the treatment given to the boundary conditions and the pile cap-pile connection by Luchesi [19] led to results closer to those of Randi [15], since the three-dimensional analyses were performed after parametric analysis of these parameters.

It is also verified by Figure 10 that the two-dimensional models of Randi [15] presented greater stiffness in relation to the reference experimental models, while the three-dimensional models presented similar stiffness. This finding highlights the importance of analyzing connections in numerical models of pile caps on piles

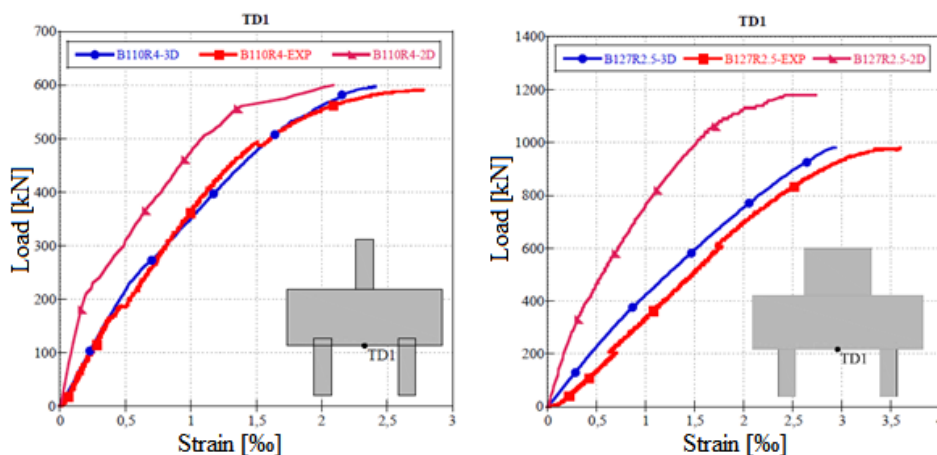


Figure 10. Load versus displacement curves of the models of series B110R4 and B127R2.5

Regarding the cracking panoramas, Munhoz [13] observed that the first visible cracks appeared in the center of the lower face of the pile caps and evolved up to half their height, with these cracks being of small magnitude and not critical. Later, cracks inclined in the direction of the compression struts appeared, characterizing the stress flow expected by the Strut-and-Tie Method. These cracks evolved to the upper and lower nodes, forming rupture planes.

Table 6 presents the results, of the experimental and numerical models, for the loads related to the first visible cracks ($F_{r,p}$), the first centered cracks ($F_{r,c}$), the first inclined cracks ($F_{r,i}$) and the maximum magnitude of the cracks in the models (w_{max}).

Table 6. Loads related to the opening of cracks and maximum cracks of the numerical models (two-dimensional and three-dimensional) and experimental models

Model	Series B110R4			
	Fr,p	Fr,c	Fr,i	wmax
	(kN)	(kN)	(kN)	(kN)
B110R4-EXP	200.00	200.00	250.00	0.50
B110R4-3D	240.20	240.20	280.00	0.52
B110R4-2D	250.00	310.00	250.00	-
Model	Series B127R2.5			
	Fr,p	Fr,c	Fr,i	wmax
	(kN)	(kN)	(kN)	(kN)
B127R2.5-EXP	247.00	247.00	383.00	0.50
B127R2.5-3D	254.55	254.55	389.30	0.40
B127R2.5-2D	330.00	425.00	395.00	-

In relation to series B110R4, for the reference experimental model the first visible cracks were centered for a load of 200.00 kN (34% of the failure load), for the three-dimensional numerical models the first visible cracks were also centered for a load of 240.2 kN (40% of the failure load). The two-dimensional model showed the first visible cracks for a load of 250.00 kN (42% of the failure load); however, these cracks were not centered, which appeared for a load of 310 kN. It is noted that inclined cracks appeared in the three models at very close loads, indicating that the numerical models presented the expected behavior according to the Strut-and-Tie Method. It is also noted that the three-dimensional numerical model presented a crack with a maximum opening of 0.52 mm, a value very close to the value of the reference experimental model.

As for series B127R2.5, it is noted that the two-dimensional numerical model of Randi [15] presented first visible cracks and first centered cracks at loads quite different from the reference experimental model. The three-dimensional model B127R2.5-3D showed very positive results compared to the experimental model and for the first visible cracks and the first inclined cracks the results show no differences and in the case of the first inclined cracks, the difference can be considered negligible.

Figure 11 presents the final cracking panoramas for models B110R4-3D, B110R4-EXP, B127R2.5-3D and B127R2.5-EXP.

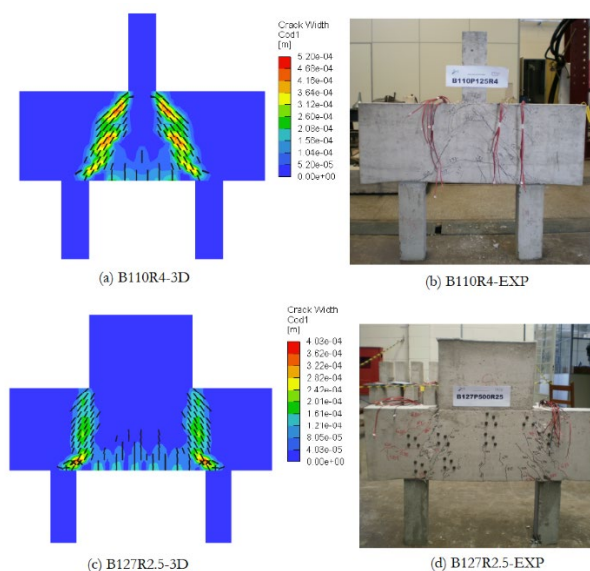


Figure 11. Cracking panoramas of the experimental and three-dimensional numerical models of pile caps on piles of series B110R4 and B127R2.5

An important aspect to be presented in this paper is the difference found in the cracking panoramas between the three-dimensional numerical models simulated with rigid connection and with interface elements in the contact between pile cap/piles. It was found that the implementation of interface elements significantly influences the formation of cracks in the pile caps on piles.

Figure 12 shows the cracks in the failure load for the lower nodal region at the connection point between pile cap-piles.

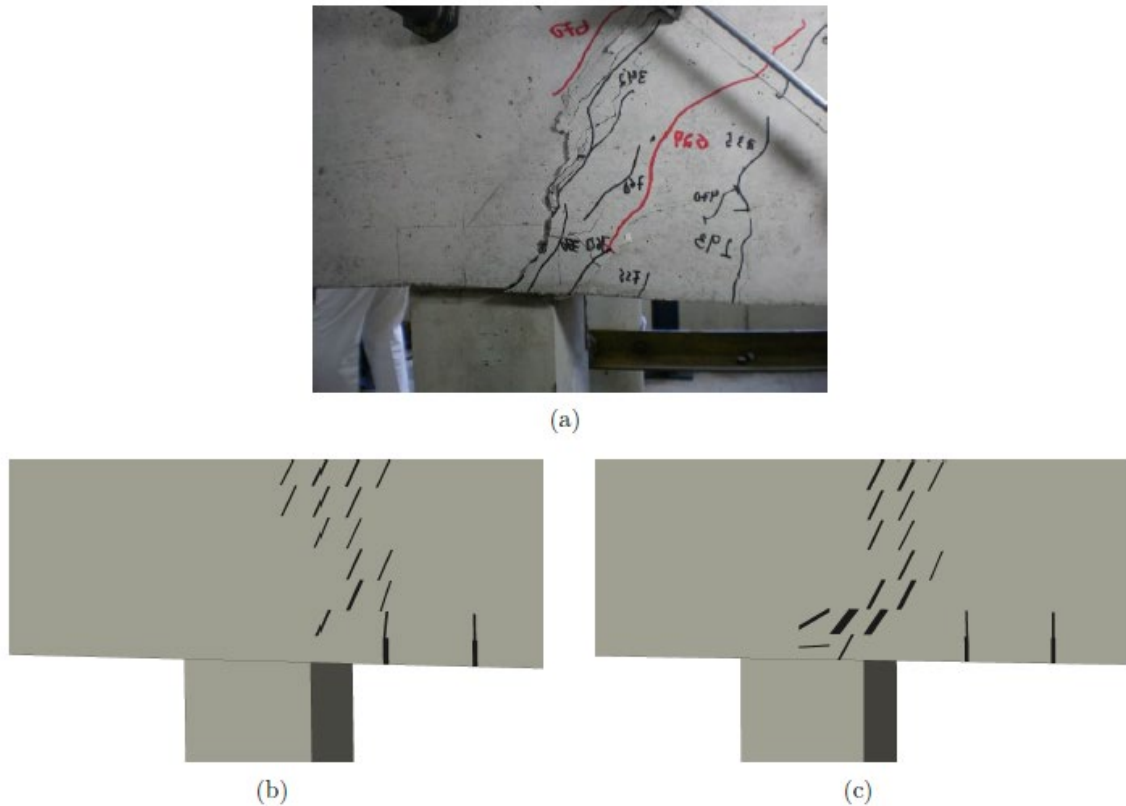


Figure 12. Crack conformation in the lower nodal region for the failure load of (a) reference experimental model, (b) numerical model with rigid connection, and (c) numerical model with interface element

It is noted, by Figure 12, that in (c) the cracks that appeared in the lower nodal region advanced over the pile head, consistently with the cracking panorama presented for the reference experimental model Figure 12 (a). The numerical model with rigid connection, Figure 12 (b), did not present this phenomenon, differentiating the behavior from that of the reference experimental model. This occurs because the rigid connection does not allow relative rotations and displacements between the points of the different connected finite elements, while the use of interface elements allows them.

This aspect is essential to improve the quality of numerical modeling of pile caps on piles, since the panorama and evolution of cracking in pile caps are well defined by the Strut-and-Tie Method, as observed by Blévet and Frémy [2] and Mautoni [3], among other authors.

5.3 Influence of pile cap width

The changes made to the pile caps to analyze the influence of pile cap width are described in item 4.2.3. The results related to failure loads, displacements and cracking panoramas will be presented.

For better understanding the variations in braking loads (F_u) and maximum displacements at failure (F_u), we present Tabel 7 with the relations of ultimate loads and maximum displacements between models C15 and C1.25 and the displacements between the models C15 and C1.25 for the failure load of models C1.25 ($F_{u1.25}$).

Table 7. Failure loads and displacements of models C1.25 and C15

Model	Fu (kN)			δFu (mm)			δFu,C1.25 (mm)	
	C1.25	C15	C15/C1.25	C1.25	C15	C15/C1.25	C15	C15/C1.25
B110R4	597.13	1039.50	1.74	2.41	3.59	1.49	1.57	0.65
B127R2.5	979.63	1638.00	1.67	2.93	2.31	0.79	0.62	0.21

By analyzing the results, we found considerable increase in the failure load of the models with greater width, in the order of 1.74 and 1.67 for series B110R4 and B127R2.5, respectively. As for displacements, it is not possible to reach a plausible conclusion about stiffness by analyzing the failure loads of the models. Thus, by analyzing the displacements of models C15 in the failure load of models C1.25, it is found that models C15 have smaller displacements, that is, they are more rigid. It is also noted that model B127R2.5 with a 15.00 cm flap showed a considerably lower displacement than the model with a 1.25 cm flap. This behavior can be explained by the fact that the column/pile cap set has a high stiffness provided, mainly, by the influence of the column cross section, which is 50.00 cm for this model.

Regarding the appearance and evolution of cracks, models C15 and C1.25 showed similar behavior, with cracks appearing on the lower face of the pile caps and evolving up to half the height of the pile caps. The inclined cracks appeared in the central region of the lateral face of the pile caps and evolved to the upper and lower nodes; an important observation is that the inclined cracks initially appeared internally in the pile caps and not in the faces, characterizing the concrete cracking effect.

Model B127R2.5C15 presented a more adequate rigid pile cap behavior when compared to model B110R4C15, due to the tie reinforcements arrangement, described in Munhoz [13].

Figure 13 shows the comparison between the cracking panoramas of the reference experimental models (C1.25) and numerical models with increased width (C15). It is noted that this comparison was performed in the failure load step of models C1.25.

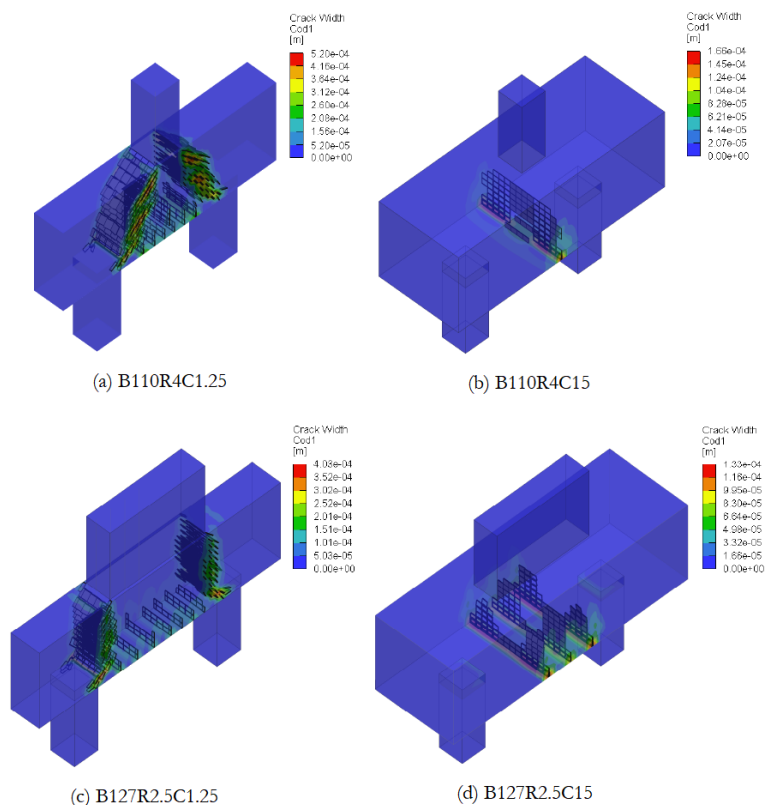


Figure 13. Internal cracking of models C1.25 (a) and (c) and models C15 (b) and (d), for the failure load of models C1.25

For the analyzed cases, it is verified that, for the same applied load, models C15 present a smaller crack opening when compared to models C1.25. This phenomenon is explained by the fact that models C15 have a greater width and, consequently, greater volume so there is a three-dimensional expansion of the tension of compression struts inside the pile cap.

This observation is important to demonstrate that there are considerable differences in the analysis of pile caps with and without side flaps. In fact, pile caps on piles are designed and executed in accordance with the normative prescriptions and indications of specialized literature and, in most cases, the recommendation to use the side flap is followed. It is important to note that, in research, there are few cases where the pile caps on piles are analyzed with the side flaps and that this parameter significantly influences the results of the tests performed.

6 CONCLUSIONS

In the process of numerically simulating pile caps supported on two piles based on the reference experimental models of Munhoz [13], we observed differences in stiffness between the models, a phenomenon also corroborated by other authors, as discussed above. We also noted the complexity of reproducing laboratory tests through numerical models, especially in the convergence of results related to displacements of the models.

The comparisons performed in this paper regarding failure loads, displacements, and cracking panoramas presented good consistency in relation to the reference experimental models.

Analysis of the results of the two-dimensional simulations performed by Randi [15] provided some disparities, especially in displacements, explained mainly by the fact that two-dimensional and three-dimensional models have different boundary conditions and values for mechanical properties of interface elements, leading to the conclusion that these factors are important in numerical modeling of pile caps on piles.

The parametric study on the connection adopted in the steel plates of the piles leads to the conclusion that, for the models analyzed here, the fixed support together with the use of interface elements between plate/piles (models CC4) presented better results when compared to the models with rigid connection. This study demonstrates that this factor is fundamental in numerical simulations.

Another important factor found is the type of connection used between pile caps/piles. Again, the use of interface elements proved more adequate than the use of rigid connections. In addition, it is concluded that the mechanical properties of the interface elements that simulate this connection is a preponderant factor in numerical models. It is also noted that inadequate definition of this connection directly affects the cracking panorama of the pile caps, mainly in the conformation region of the lower node.

The models simulated with side flap of the pile caps had significantly higher failure loads than the models with no side flap. We also found that pile caps with greater width are more rigid. The models with smaller width showed intense crack opening, unlike the other models that showed only bending cracks on the lower face of the pile caps. It is also noted that the increased width of the pile caps enabled greater propagation of the compressive stress of the struts inside the pile cap, since there is more concrete volume for this phenomenon to occur. These observations prove the influence of pile cap width on its behavior.

Finally, it is concluded that the boundary conditions, use of interface elements to simulate the contact between different materials and concreting joints and pile cap width are important factors that significantly change the stiffness of the models simulated numerically.

ACKNOWLEDGEMENTS

I acknowledge the School of Civil Engineering, Architecture and Urbanism at the State University of Campinas, and the Department of Structures and its professors for their support and for making available the tools and computational programs that made this research feasible.

REFERENCES

- [1] Associação Brasileira de Normas Técnicas, *Projeto de Estruturas de Concreto: Procedimento, NBR6118:2014*, 2014.
- [2] J. Blévoit and R. Frémy, "Semelles sur pieux," *Annales Inst. Technique Batiment Trav. Publics*, vol. 20, no. 230, pp. 223–295, Feb 1967.
- [3] M. Mautoni, *Blocos Sobre Dois Apoios*. São Paulo: Grêmio Politécnico, 1972.
- [4] H. P. J. Taylor and J. L. Clarke, "Some detailing problems in concrete frame structures," *Struct. Eng.*, vol. 54, no. 1, pp. 19–32, Jan 1976.

- [5] P. Adebar, D. Kuchma, and M. P. Collins, "Strut-and-tie modelos for the desin of pile caps: An experimental study," *ACI J.*, vol. 87, pp. 81–91, Jan/Feb 1990.
- [6] J. Schlaich and K. Schafer, "Design and detailing of structural concrete using strut-and-tie models," *Struct. Eng.*, vol. 69, no. 6, pp. 113–125, Mar 1991.
- [7] C. Sam and P. K. Iyer, "Nonlinear finite element analysis of reinforced concrete four pile caps," *Comput. Struc.*, vol. 571, no. 4, pp. 605–622, 1995.
- [8] American Concrete Institute, *Building Code Requirements for Reinforced Concrete, ACI 318:19*, 2019.
- [9] CEB-FIP, *Model Code 2010*. Lausanne, Switzerland: Comité Euro-Internacional du Béton, 2010.
- [10] Canadian Portland Cement Association, *Design of Concrete Structures with Explanatory Notes, CSA STANDARD A23.3 2019*, 2019.
- [11] R. G. Delalibera, "Análise experimental e numérica de blocos de concreto armado sobre duas estacas submetidos à ação de força centrada e excêntrica," Ph.D. dissertation, EESC/USP, São Carlos, Brasil, 2006.
- [12] T. E. T. Buttignol, "Análise Computacional de Blocos sobre Estacas," M.S. thesis, FEC, Unicamp, Campinas, Brasil, 2011.
- [13] F. S. Munhoz, "Análise experimental e numérica de blocos rígidos sobre duas estacas com pilares de seções quadradas e retangulares e diferentes taxas de armadura," Ph.D. dissertation, EESC/USP, São Carlos, Brasil, 2014.
- [14] R. Barros, R. G. Delalibera, and J. S. Giongo, "Avaliação experimental e numérica de blocos de concreto armado sobre duas estacas," *Revista Portuguesa de Engenharia de Estruturas*, vol. 1, pp. 43–54, July 2016.
- [15] R. P. Randi, "Influência do comprimento de ancoragem das armaduras do pilar em blocos sobre duas estacas," M.S. thesis, FEC, Unicamp, Campinas, Brasil, 2017.
- [16] T. E. T. Buttignol and L. C. Almeida, "Análise numérica tridimensional de blocos sobre duas estacas," *Rev. Ibracon Estrut. Mater. Brasil*, vol. 5, no. 2, pp. 252–283, Apr 2012.
- [17] R. P. Randi, L. C. Almeida, L. M. Trautwein, and F. S. Munhoz, "Análise da influência do comprimento de ancoragem da armadura do pilar no bloco sobre duas estacas," *Rev. Ibracon Estrut. Mater. Brasil*, vol. 11, no. 5, pp. 1122–1150, Oct 2018.
- [18] Associação Brasileira de Normas Técnicas. *Projeto de Estruturas de Concreto: Procedimento, NBR 6118:2003*, 2003.
- [19] G. L. Luchesi, "Análise numérica tridimensional de blocos de fundação apoiados sobre duas estacas," M.S. thesis, FEC, Unicamp, Campinas, SP, 2020.
- [20] V. Cervenka and V. K. Papanikolaou, "Three dimensional combined fracture–plastic material model for concrete," *Int. J. Plast.*, vol. 12, no. 4, pp. 2192–2220, 2008.
- [21] P. Menetrey and J. K. Willian, "Triaxial failure criterion for concrete and its generalization," *ACI Struct. J.*, vol. 92, no. 6, pp. 642, 1995.
- [22] Y. R. Rashid, "Ultimate strength analysis of prestressed concrete pressure vessels," *Nucl. Eng. Des.*, vol. 7, no. 7, pp. 334, 1968.
- [23] Z. P. Bazant and B. H. Oh, "Crack band theory for fracture of concrete," *Matériaux et Construction*, vol. 16, no. 3, p. 155–177, 1983.
- [24] W. J. M. Rankine, *Manual of Applied Mechanics*. Glasgow, Scotland: Griffin, 1876.
- [25] D. A. Hordijk, "Local approach to fatigue of concrete," Ph.D. dissertation, Delft University of Technology, The Netherlands, 1991.
- [26] V. Cervenka, L. Jandele, and J. Cervenka, *Atena Program Documentation, Part I: Theory*. Prague, Republic Czech: Cervenka Consulting, 2018. 304 p.
- [27] U. R. Alonso, *Exercícios de Fundações*. São Paulo, Brasil: Edgar Blucher, 1983.

Author contributions: GLL: conceptualization, methodology, formal analysis, data curation; RPR: conceptualization, data curation, writing; LMT and LCA: resources, funding acquisition, supervision.

Editors: José Marcio Calixto, Guilherme Aris Parsekian.